

Full Wavefield Migration by Inversion

Shaoping Lu, Faqi Liu, Nizar Chemingui and Mikhail Orlovich, PGS*

Summary

Conventional seismic processing treats high-order reflected events as noise and tremendous efforts have been spent on their removal. Because of the extra interactions with the subsurface, multiples can be used as effective signal. When combined properly, the full wavefield including primaries and high-order reflections can significantly improve the illumination of the subsurface compared to primaries only. However, crosstalk has always been a major challenge for the joint imaging algorithm. In this paper, we present a Least-Squares inversion solution for depth imaging of the full recorded wavefield. The method effectively reduces the crosstalk and enhances the resolution by fully taking advantage of the extended illumination of all orders of reflections present in the data.

Introduction

Separated Wavefield IMaging (SWIM) produces images with improved illumination and resolution by utilizing sea-surface reflected multiple energy (Lu et al., 2015). Full Wavefield Migration (FWM) images both primaries and multiples simultaneously, and potentially yields improved images in comparison to either migration of primaries or multiples only. Figure 1 illustrates the concepts behind primary imaging, SWIM and FWM respectively. The images are produced using the SEAM Phase I model with the sparse shot acquisition geometry on a 600m by 600m grid. The image of primaries [Figure 1D] has shallow illumination challenges due to the sparse shot distribution. SWIM greatly enhances the shallow imaging illumination by converting each receiver to a virtual source [Figure 1E]. At larger depths, however, the SWIM image quality diminishes due to less of recorded surface multiple energy, given limited recording time and acquisition offset. FWM delivers the overall optimal result by combining the illumination from both primary and multiple reflections [Figure 1F].

In practice, perfect balancing of the reflected energy remains challenging when one images the full wavefiled using a standard migration operator with virtual sources. In addition, given the blending nature of the FWM algorithm, the image contains crosstalk artifacts. These artifacts can be attenuated via a deconvolution imaging condition (Lu et al., 2015) or a crosstalk prediction and subtraction workflow (Lu et al., 2016). However, both strategies are sub-optimal, as the crosstalk in FWM is created by the interference in the blended migration algorithm. Conversely, the inversion algorithm solves a Least-Squares minimization problem, which excludes the interference terms existing in a one-step

migration (Davydenko and Verschuur, 2014; Tu, 2015; Lu et al., 2018). Least-Squares Full Wavefield Migration (LS-FWM) computes a reflectivity image that explains the observed data without involving interference noise, and automatically balances the contribution from each component (primaries and all orders of multiple reflections).

We therefore propose a Least-Squares inversion scheme for full wavefield migration. The algorithm solves for the earth reflectivity by means of data residual reduction in an iterative fashion. The method has been applied to both synthetic and field data examples with great results.

Theory

Compared to primary imaging where the source is an impulse, FWM uses a non-transient signal as boundary source wavefield. Therefore, imaging the full wavefield by using a standard migration algorithm can generate crosstalk noise in the image (Lu et al., 2016).

During FWM, the source wavefield, S , gets extrapolated forward $P_s = w_s S$ and the receiver wavefield, R , is extrapolated backward $P_r = w_r^* R$. Here, P_s and P_r are the source and receiver wavefields at the subsurface; w_s and w_r are the extrapolators for the source and receiver wavefields. In a standard FWM, an image, m , is created by cross-correlating the two wavefields, at the subsurface:

$$m = P_s^* P_r. \quad (1)$$

However, the exact solution for m should be computed as:

$$m = (w_r^* w_r)^{-1} \frac{P_s^* P_r}{P_s^* P_s}, \quad (2)$$

which is the inverse of the forward modeling process.

Comparing to equation 1, we find that a cross-correlation imaging condition only kinematically matches the solution in equation 2. Therefore, it is not capable to produce an optimal image in FWM.

In the case where the subsurface is close to a 1D model, equation 2 can be approximated as:

$$m = \frac{P_s^* P_r}{P_s^* P_s}. \quad (3)$$

Full Wavefield Migration by Inversion

Equation (3) is the deconvolution imaging condition. Lu et al. (2015) have demonstrated that it works reasonably well in non-complex regimes, where $w_r^* w_r$ is close to unitary.

To estimate equation 2 correctly, a Least-Squares based inversion solution is proposed to approximate the earth reflectivity, which can explain the boundary observation without having crosstalk in \mathbf{m} .

We implement an iterative inversion scheme in a migration/demigration framework. Each inversion iteration consists of one Born modeling (Cohen et al., 1966) and one migration. Advanced regularization techniques are also employed to composite an efficient and stable migration inversion algorithm (Lu et al., 2018).

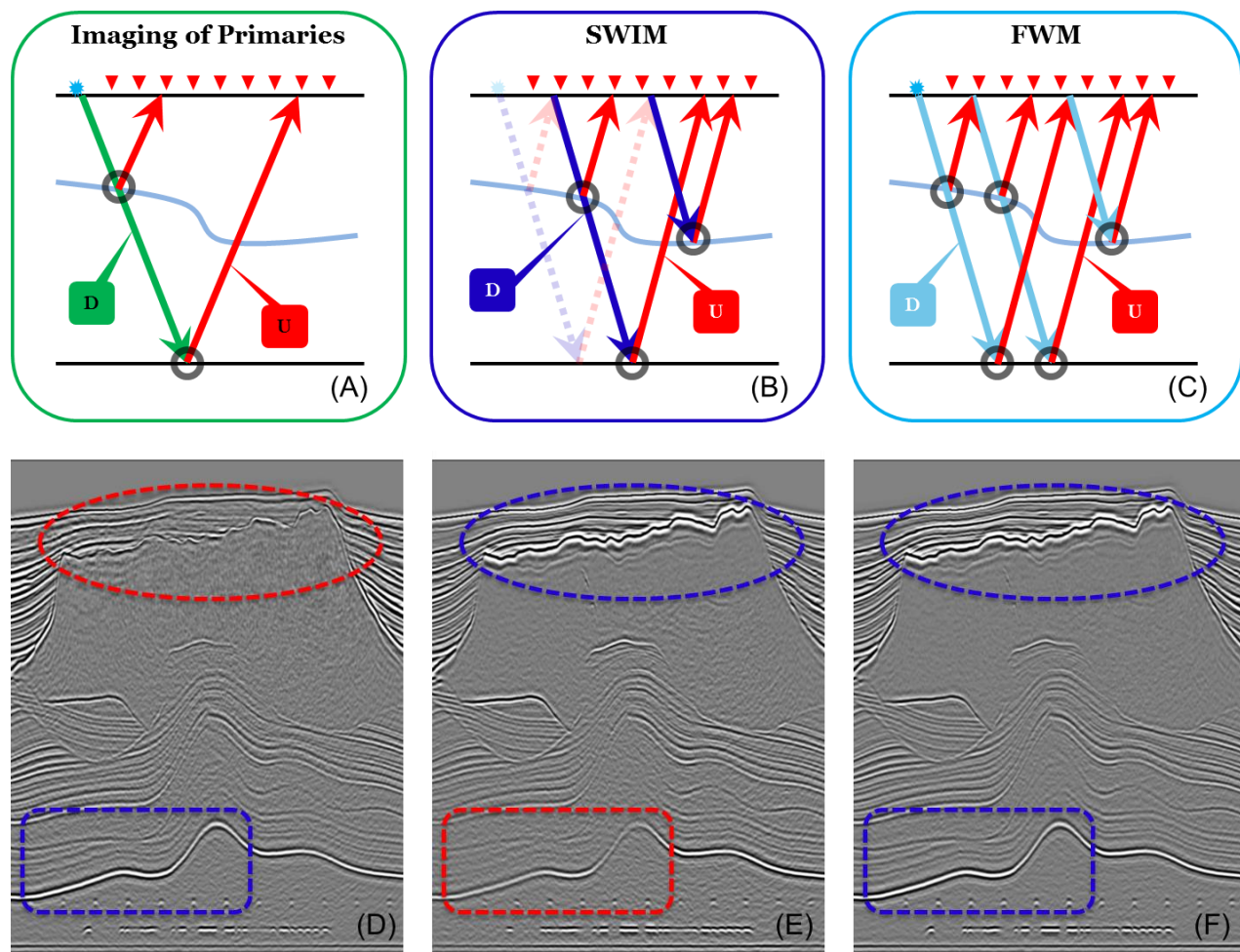


Figure 1. (Upper) Schematic illustrations of Imaging of Primaries (A), SWIM (B), and FWM (C); and (Lower) Equivalent synthetic SEAM Phase I model images. The sparse shot acquisition geometry has 2793 shots on a 600m by 600m grid. Imaging of Primaries has better deep target illumination (D), SWIM has better shallow target imaging (E), and FWM provides the best imaging at all depths (F).

Synthetic and Field Data Examples

We have applied LS-FWM to the 2D Sigsbee2b synthetic dataset and compared the LS-FWM result with FWM

images using cross correlation and deconvolution imaging conditions. Figure 2 displays a subsection of the images to show the effects of deconvolution imaging condition and Least-Squares migration upon crosstalk attenuation.

Full Wavefield Migration by Inversion

In the FWM result using a cross correlation imaging condition [Figure 2A], the strong crosstalk is related to the interference of major reflection events, such as the water bottom, salt flanks and diffraction. The deconvolution imaging condition attenuates most of the flat crosstalks [Figure 2B]. However, the deconvolution imaging condition alone cannot attenuate either the very strong coherent interference or the non-flat crosstalks. The LS-FWM approximates the analytic solution in equation 2, and further reduces the crosstalk in the image.

We also investigated the algorithm on a subset (428 receivers) of an ocean bottom survey in a shallow water environment. The down-going pressure data from P-Z subtraction is used for FWM and LS-FWM. In this case, the images combine both the mirrored primary component and higher orders of surface reflected energy. The depth slices displayed in figure 3 show resolution improvement

by using a deconvolution imaging condition [Figure 3B] and the Least-Squares full inversion solution [Figure 3C]. The crosstalks in FWM result contaminate the imaging resolution, the deconvolution imaging condition increases vertical resolution, and the LS-FWM solution balances the amplitude illumination and enhances resolution in both vertical and lateral directions (e.g. fault).

Besides the resolution improvement, the effects of deconvolution and Least-Squares migration to crosstalk attenuation are demonstrated in the vertical sections in Figure 4. The FWM image with cross correlation imaging condition is covered by strong crosstalks [Figure 4A]. The deconvolution imaging condition is capable of attenuating many interference events in the image while leaving some coherent residuals (indicated by red arrows in figure 4B). The LS-FWM suppresses the residual crosstalk and produces even cleaner results [Figure 4C].

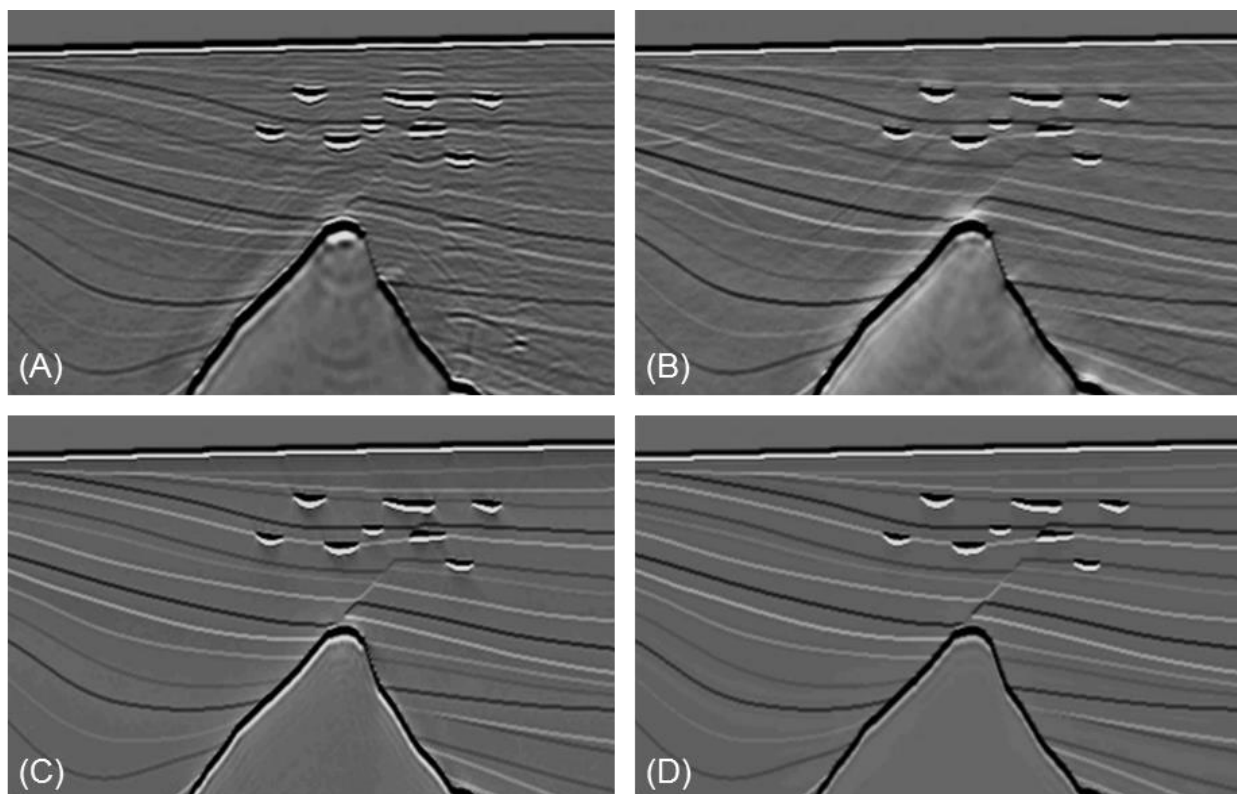


Figure 2, a subsection from the 2D Sigsbee2b synthetics. (A) FWM image with cross correlation imaging condition; (B) FWM image with deconvolution imaging condition; (C) LS-FWM image; (D) bandlimited reflectivity model.

Full Wavefield Migration by Inversion

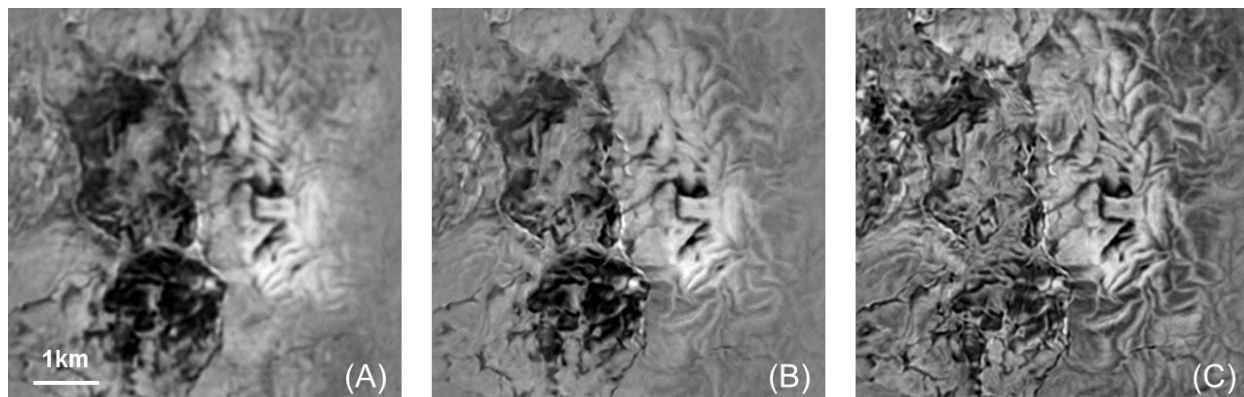


Figure 3, depth slices (1300m) from a shallow water OBC data: (A) FWM image with cross correlation imaging condition, (B) FWM image with deconvolution imaging condition, (C) LS-FWM image.

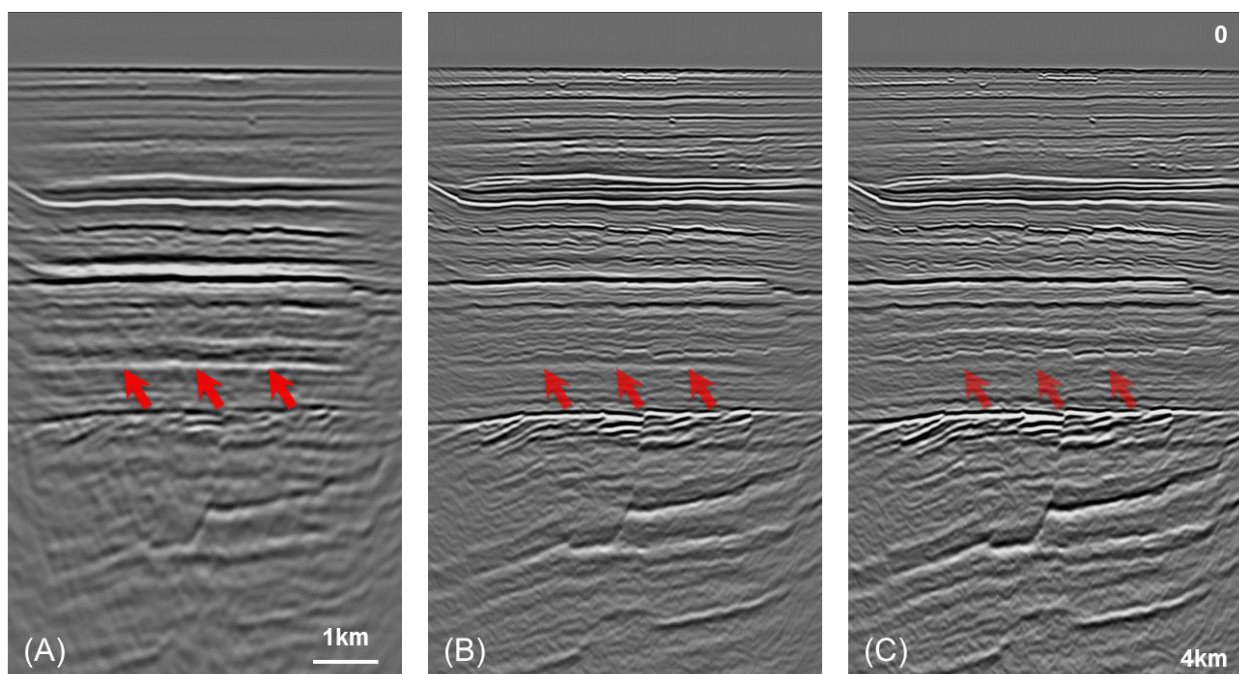


Figure 4, inline images from a shallow water OBC data: (A) FWM image with cross correlation imaging condition, (B) FWM image with deconvolution imaging condition, (C) LS-FWM image. Red arrows indicate crosstalk.

Conclusions

We present a Least-Squares algorithm for Full Wavefield Migration (LS-FWM) that addresses the crosstalk problem in FWM and effectively images the full reflected wavefield including primaries and multiples. Successful applications to both synthetic and field data examples demonstrate that LS-FWM greatly improves the illumination and resolution of the seismic images.

Acknowledgements

The authors would like to thank PGS for permission to publish this work and our colleagues Julien Oukili and Grunde Rønholz for their support. We thank Statoil AS, the Snorre license partners Petoro AS, ExxonMobil E&P Norway AS, Idemitsu Petroleum Norge AS, DEA Norge AS and Point Resources AS. The views and opinions expressed in this paper are those of the authors and are not necessarily shared by the license partners.

REFERENCES

- Cohen, J., F. Hagin, and N. Bleistein, 1986, Three-dimensional Born inversion with an arbitrary reference: *Geophysics*, **51**, 1552–1558, <https://doi.org/10.1190/1.1442205>.
- Davydenko, M., and D. J. Verschuur, 2014, Full wavefield migration in three dimensions: 84th Annual International Meeting, SEG, Expanded Abstracts, 3935–3940, <https://doi.org/10.1190/segam2014-1079.1>.
- Lu, S., F. Liu, N. Chemingui, A. Valenciano, and A. Long, 2018, Least-squares full-wavefield migration: *The Leading Edge*, **37**, 46–51, <https://doi.org/10.1190/tle37010046.1>.
- Lu, S., D. Whitmore, A. Valenciano, and N. Chemingui, 2015, Separated-wavefield imaging using primary and multiple energy: *The Leading Edge*, **34**, 770–778, <https://doi.org/10.1190/tle34070770.1>.
- Lu, S., D. Whitmore, A. Valenciano, N. Chemingui, and G. Ronholt, 2016, A practical crosstalk attenuation method for separated wavefield imaging: 86th Annual International Meeting, SEG, Expanded Abstracts, 4235–4239, <https://doi.org/10.1190/segam2016-13849878.1>.
- Tu, N., 2015, Fast imaging with surface-related multiples: Ph.D. thesis, The University of British Columbia.